Dynamical motion of atoms in surfaces: A model of W (100) as an example

J. E. Black,* Bernardo Laks,† and D. L. Mills
Department of Physics, University of California, Irvine, California 92717
(Received 28 February 1980)

For a model of the (100) surface of tungsten, we have studied the mean-square displacement of atoms and its anisotropy as a function of distance from the surface. In addition, we study correlations in the motion of nearest and next-nearest neighbors in and near the surface. These calculations employ the continued-fraction method to construct the relevant spectral densities. We assess the accuracy and efficiency of the method, and analysis of the structures in the various spectral-density functions provides insight into the modes which control displacement amplitudes and correlations in the surface.

I. INTRODUCTION

While the lattice dynamics of crystal surfaces has been an active topic of theoretical study during the past decade,[1] rather little detailed data are available on clean crystal surfaces. For example, considerable attention has been devoted to the theoretical analysis of surface contributions to the specific heat, and the few experiments available are in qualitative accord with theory, but examples of meaningful quantitative contact are sparse.[2] Information on the mean-square displacement in the surface can be extracted from the temperature variation of low-energy-electron diffraction (LEED) data, although the procedure used to extract information from the data may well lead to significant quantitative errors on the order of ten or twenty percent.[3]

At present, electron spectrometers with energy resolution sufficient to study phonons at surfaces through high-resolution electron-energy-loss spectroscopy (EELS) are either operational or under construction in many laboratories. To date, most EELS experiments explore the vibrational motions of adsorbates on the surface,[4] though there are notable exceptions.[5] We are particularly intrigued by the beautiful experiment reported recently by Ibach and Bruchmann,[6] which through analysis of an EELS spectrum of an adsorbate-covered Ni (111) surface provides information on the frequency of a zone-boundary Rayleigh surface phonon. In the near future we can expect experiments such as this one to provide information on the frequencies that control atomic motions in surfaces. There is thus need for further theoretical development which focuses not only on thermodynamic effects of the surface and the mean-square displacement there, but also on the frequency spectra of the surface atoms and correlations between these motions.

The purpose of this paper is to present a series of such calculations for a model of the W (100) surface. We do this through application of a method introduced by Cyrot-Lackmann and her colleagues in the study of the electronic structure of transition-metal surfaces,[7] but which has not been applied extensively to problems in surface lattice dynamics.[8] This is the continued-fraction method. Specifically, we consider correlation functions of the form $\langle u_\alpha(\vec{l})u_\beta(\vec{l}')\rangle$, where $u_\alpha(\vec{l})$ is the αth Cartesian component of displacement of the atom at site $\vec{l}$. With the choice $\alpha=\beta$, $\vec{l}=\vec{l}'$, we have a component of the mean-square displacement of the atom at site $\vec{l}$. For such correlation functions we may introduce a spectral density function $\rho_{\alpha\beta}(\vec{l},\vec{l}';\omega)$ to write

$$\langle u_\alpha(\vec{l})u_\beta(\vec{l}')\rangle = \frac{\hbar}{2M}\int_0^\infty \frac{d\omega}{\omega}\,(1+2\bar{n}_\omega)\rho_{\alpha\beta}(\vec{l},\vec{l}';\omega)\,, \tag{1.1}$$

with M the mass of the atoms and $\bar{n}_\omega=[\exp(\hbar\omega/k_BT)-1]^{-1}$ the Bose-Einstein function. We use the continued-fraction method to construct the spectral-density function, then we calculate the correlation function by performing the integration on frequency in Eq. (1.1). As we shall see, study of the spectral-density functions provides considerable insight into the characteristic frequencies and phonon modes that control particular atomic motions in the surface. Before we turn to a discussion of the method and a presentation of our results, we comment on the reasons why we have chosen to use the continued-fraction approach.

In theoretical studies of the lattice dynamics of surfaces, it has become usual to proceed as follows.[1] One considers not a semi-infinite crystal, but rather a finite slab semi-infinite in two directions (the x and y directions), with a finite number N of layers in the z direction, which is normal to the surface. In practice, N may range from 10 to 20. Periodic boundary conditions are applied in the x and y directions while the atoms in the outermost layers have a local environment identical to atoms in the surface of a

semi-infinite crystal.[9] Then for such a system, translational symmetry in the x and y direction renders $\vec{k}_{\parallel}$, the component of wave vector parallel to the surface, a good quantum number. Thus, one seeks eigensolutions of the equation of motion in the form $u_\alpha(\vec{l}) = \exp(i\vec{k}_{\parallel}\cdot\vec{l}_{\parallel})u_\alpha(l_z)$ with $\vec{l} = \vec{l}_{\parallel} + \hat{z}l_z$ and $\vec{l}_{\parallel}$ the projection of $\vec{l}$ onto the xy plane. For a monatonic crystal, for each $\vec{k}_{\parallel}$, one diagonalizes a $3N \times 3N$ dynamical matrix to find the set of eigenfrequencies and eigenvectors. Finally, to calculate a correlation function such as $\langle u_\alpha(\vec{l})u_\beta(\vec{l}')\rangle$, one must integrate the appropriate combination of eigenfrequencies and eigenvectors over the two-dimensional Brillouin zone. For each $\vec{k}_{\parallel}$ included in the numerical integration, the $3N \times 3N$ dynamical matrix must be diagonalized.

From our point of view, the slab method has a number of disadvantages. First of all, essential use is made of the translational symmetry parallel to the surface. Of course, a perfectly smooth, ideal crystal surface has precisely such translational symmetry. In the near future, we shall direct our attention to localized perturbations on the surface such as an isolated adsorbate atom. In such a problem the translational symmetry is now lost, and it is difficult to envision application of the approach outlined in the preceding paragraph to this important class of problems. As others have emphasized,[7] the continued-fraction method is a "real-space" method that makes no use of Brillouin zones or wave vectors. As a consequence, it can be applied to surfaces perturbed by localized defects with no more difficulty than encountered in studying the perfect surface. In the present paper, we concentrate on a perfect-crystal surface so that our calculations may be compared directly with earlier studies of the same surface by the slab method to see if the continued-fraction method reproduces these results.

There is a problem of principle with the slab method that may be stated as follows. It is well known that for a two-dimensional layer of atoms with displacement $\vec{u}(\vec{l})$ confined to the plane, the mean-square displacement $\langle u^2\rangle$ diverges as the transverse dimensions L_x and L_y of the layer are allowed to become infinite. If we consider a slab with a finite number of layers N and let L_x and L_y become infinite, $\langle u^2\rangle$ diverges again because to a long-wavelength acoustical phonon, the slab is indistinguishable from a single atomic layer of suitable mass density[10] in the limit $|\vec{k}_{\parallel}|d \ll 1$, where d is the slab thickness and $|\vec{k}_{\parallel}|$ is the wave vector of the phonon. Thus, for a slab with a fixed number of layers, one finds that as the number of points in the two-dimensional Brillouin zone is increased in a numerical calculation, $\langle u^2\rangle$ necessarily increases without bound. In practice, the number of $\vec{k}_{\parallel}$ points is chosen to correspond roughly to a cube, with periodic boundary conditions applied in the $\hat{x}$ and $\hat{y}$ directions and true surfaces perpendicular to $\hat{z}$. Then an attempt to improve accuracy by using a finer mesh in the two-dimensional Brillouin zone requires one to increase the number of layers N simultaneously to avoid the divergence. In a practical calculation this becomes costly, since the time required to diagonalize the $3N \times 3N$ matrix scales as N^3 for typical computer routines. The cost of the calculation then scales as N^5 overall. This divergence is a special feature of lattice dynamics, and there is no analog in the electronic structure problem, where many groups also use slab methods.

The continued-fraction method allows us to work with a truly semi-infinite geometry for which no such divergences occur. If results of high accuracy are desired, we also believe it much more efficient than the slab method, though we claim no greater accuracy in our calculations of *static* correlation functions such as $\langle u_\alpha(\vec{l})u_\beta(\vec{l}')\rangle$. We do believe the continued-fraction method does a superior job of providing the spectral densities $\rho_{\alpha\beta}(\vec{l},\vec{l}';\omega)$, which will be required in the analysis of EELS data. We are frankly impressed by the results we have obtained, which seem very reliable, save in the low-frequency limit, where the fact that one samples a finite cluster of atoms limits one's ability to obtain proper behavior for the spectral density. The reader may compare the results and calculations reported here with an early paper by Roundy and Mills,[11] which in essence calculates certain spectral densities by the slab method. Only rather crude histograms were reported by Roundy and Mills, and while the information that emerged from their slab calculation might have been processed more optimally, it is hard for us to see how results as detailed as those reported here could be obtained without a major increase in computing time.

The flexibility of the continued-fraction method, and the reliable spectral densities that can be obtained with it, suggests to us that it should be more widely used in studies of the lattice dynamics of crystal surfaces. We now turn to a discussion of the method, to our results, and the conclusions that follow.

II. GENERAL DISCUSSION AND THE METHOD OF CALCULATION

We begin by writing down a number of general relationships that enter the description of the lattice dynamics (in the harmonic approximation) of an array of N particles, each with mass M.

The aim of the introductory remarks is to establish our notation and also to make contact with earlier applications of the method of continued fractions to problems in the electronic structure of surfaces. The opening remarks cover well-trodden ground, but for clarity we wish to summarize the basic structure of the theory.

If $u_\alpha(\vec{l})$ is the αth Cartesian component of the displacement $\vec{u}(\vec{l})$ of the mass at lattice site $\vec{l}$ from its equilibrium position, then $u_\alpha(\vec{l})$ obeys the equation of motion

$$\ddot{u}_\alpha(\vec{l}) + \sum_\beta \sum_{\vec{l}'} D_{\alpha\beta}(\vec{l},\vec{l}')u_\beta(\vec{l}') = 0\,, \tag{2.1}$$

where one may construct the dynamical matrix $D_{\alpha\beta}(\vec{l},\vec{l}')$ from knowledge of the interatomic potential.[1] If ω_s is the frequency of the sth normal mode of the system and $e_\alpha^{(s)}(\vec{l})$ is the associated eigenvector normalized so that

$$\sum_\alpha \sum_{\vec{l}'} |e_\alpha^{(s)}(\vec{l})|^2 = 1\,, \tag{2.2}$$

one extracts ω_s and $e_\alpha^{(s)}(\vec{l})$ from the eigenvalue equation

$$\omega_s^2 e_\alpha^{(s)}(\vec{l}) = \sum_\beta \sum_{\vec{l}'} D_{\alpha\beta}(\vec{l},\vec{l}')e_\beta^{(s)}(\vec{l}')\,. \tag{2.3}$$

Since the matrix $D_{\alpha\beta}(\vec{l},\vec{l}')$ is Hermitian by virtue of the relation $D_{\alpha\beta}(\vec{l},\vec{l}') = D_{\beta\alpha}(\vec{l}',\vec{l})$,[1] ω_s^2 is necessarily real, and $e_\alpha^{(s)}(\vec{l})$ may be chosen real also. The eigenvectors then satisfy an orthonormality relation which may be written

$$\sum_\alpha \sum_{\vec{l}} e_\alpha^{(s)}(\vec{l})e_\alpha^{(s')}(\vec{l}) = \delta_{ss'} \tag{2.4}$$

and a closure relation that reads

$$\sum_s e_\alpha^{(s)}(\vec{l})e_\beta^{(s)}(\vec{l}') = \delta_{\alpha\beta}\delta_{\vec{l}\vec{l}'}\,, \tag{2.5}$$

where in these statements $\delta_{\alpha\beta}$, $\delta_{ss'}$, and $\delta_{\vec{l}\vec{l}'}$ are Kronecker delta functions.

Upon quantizing the vibrational motions of the array of masses, one finds the correlation functions $\langle u_\alpha(\vec{l})u_\beta(\vec{l}')\rangle$ between displacements associated with the mass at $\vec{l}$ and that at $\vec{l}'$ may be written[1]

$$\langle u_\alpha(\vec{l})u_\beta(\vec{l}')\rangle = \sum_s \frac{\hbar}{2M\omega_s} e_\alpha^{(s)}(\vec{l})e_\beta^{(s)}(\vec{l}')(1+2\bar{n}_s)\,. \tag{2.6}$$

We have assumed the system is in thermal equilibrium at temperature T, so $\bar{n}_s = [\exp(\hbar\omega_s/k_BT) - 1]^{-1}$ is the Bose-Einstein function which gives the number of thermally excited quanta associated with the mode of frequency ω_s.

For our purposes, it will prove convenient to introduce the Green's function $U_{\alpha\beta}(\vec{l},\vec{l}';z)$ defined by the relation

$$U_{\alpha\beta}(\vec{l},\vec{l}';z) = \sum_s \frac{e_\alpha^{(s)}(\vec{l})e_\beta^{(s)}(\vec{l}')}{\omega_s^2 - z^2}\,. \tag{2.7}$$

It is this quantity we shall calculate by means of the method of continued fractions. From $U_{\alpha\beta}(\vec{l},\vec{l}';z)$ we may introduce the spectral-density function, with ϵ a positive infinitesimal,

$$\rho_{\alpha\beta}(\vec{l},\vec{l}';\omega) = \frac{\omega}{i\pi}\,[U_{\alpha\beta}(\vec{l},\vec{l}';\omega+i\epsilon) - U_{\alpha\beta}(\vec{l},\vec{l}';\omega-i\epsilon)] \tag{2.8a}$$

$$\equiv \sum_s e_\alpha^{(s)}(\vec{l})e_\beta^{(s)}(\vec{l}')\delta(\omega-\omega_s)\,, \tag{2.8b}$$

which enables the correlation function in Eq. (2.6) to be written

$$\langle u_\alpha(\vec{l})u_\beta(\vec{l}')\rangle = \int_0^\infty d\omega \frac{\hbar}{2M\omega}(1+2\bar{n}_\omega)\rho_{\alpha\beta}(\vec{l},\vec{l}',\omega)\,. \tag{2.9}$$

The function $\rho_{\alpha\beta}(\vec{l},\vec{l}';\omega)$ provides information on the characteristic frequencies which contribute to correlations between the displacements $u_\alpha(\vec{l})$ and $u_\beta(\vec{l}')$. Consider as a special case the autocorrelation function $\langle u_\alpha^2(\vec{l})\rangle$ which gives the mean-square displacement of the atom on site $\vec{l}$ in the Cartesian direction α. Deep in the bulk of a crystal of cubic symmetry, $\langle u_x^2(\vec{l})\rangle$, $\langle u_y^2(\vec{l})\rangle$, and $\langle u_z^2(\vec{l})\rangle$ are necessarily equal and independent of $\vec{l}$. One then easily sees that

$$\rho_{xx}(\vec{l},\vec{l};\omega) = \rho_{yy}(\vec{l},\vec{l};\omega) = \rho_{zz}(\vec{l},\vec{l};\omega) = \tfrac{1}{3}\rho_{\rm tot}(\omega)\,, \tag{2.10}$$

where $\rho_{\rm tot}(\omega)$ is the density of phonon modes per atom in the bulk, normalized so that

$$\int_0^\infty d\omega\,\rho_{\rm tot}(\omega) = 3\,, \tag{2.11}$$

where the factor of 3 on the right-hand side of Eq. (2.11) arises because each atom has 3 degrees of freedom.

As we move from the bulk of the crystal toward the surface, we may think of $\rho_{xx}(\vec{l},\vec{l};\omega)$, $\rho_{yy}(\vec{l},\vec{l};\omega)$, and $\rho_{zz}(\vec{l},\vec{l};\omega)$ as effective local phonon densities of states which describe the composition in frequency of motions of the atoms in the x, y, and z directions, respectively. Near the surface, the three directions are no longer equivalent by symmetry, of course, so these three functions will in general be different. Finally, for $\vec{l}\neq\vec{l}'$, $\rho_{\alpha\beta}(\vec{l},\vec{l}';\omega)$ is a generalization of the notion of a local density of states. Generally speaking, we refer to $\rho_{\alpha\beta}(\vec{l},\vec{l}';\omega)$ as a spectral density which may differ dramatically near the surface from the form appropriate to the bulk of the crystal.

We may make direct contact between $U_{\alpha\beta}(\vec{l},\vec{l}';z)$ and the Green's functions which enter the theory of electronic energy levels in crystals in the tight-

binding limit. We have $3N$ degrees of freedom in the system of N masses, and we introduce a $3N$-dimensional column vector $|\vec{l}\alpha\rangle$ which has zeros everywhere save for a single entry of unity at that position which corresponds to motion in the Cartesian direction α of the atom at site $\vec{l}$. If $\underline{D}$ is the dynamical matrix in the $3N \times 3N$ space spanned by the set $|\vec{l}\alpha\rangle$, then we have

$$U_{\alpha\beta}(\vec{l}, \vec{l}'; z) = \left\langle \vec{l}\alpha \left| \frac{1}{\underline{D} - z^2 \underline{I}} \right| \vec{l}'\beta \right\rangle . \tag{2.12}$$

By comparing Eq. (2.12) with Eq. (1.1) of the paper by Haydock, Heine, and Kelly,[12] we see there is a one-to-one correspondence between lattice dynamics and the tight-binding description of electron energy levels of solids if we consider a tight-binding problem with p orbitals associated with each atomic site. In place of the tight-binding Hamiltonian, we have the dynamical matrix $\underline{D}$, and in place of the electronic energy E we have z^2. Finally, $U_{\alpha\beta}(\vec{l}, \vec{l}'; z)$ differs from the conventional definition of the electron Green's function by an overall sign. These remarks enable us to take the method of continued fractions as developed in the electronic structure literature directly over to the problem of surface lattice dynamics.

To recall the general structure of the continued-fraction method, consider first the diagonal elements $U_{\alpha\alpha}(\vec{l}, \vec{l}; z)$ used to form the spectral density for calculating the mean-square displacement. In our case, this may be written

$$U_{\alpha\alpha}(\vec{l}, \vec{l}; z) = \cfrac{1}{z^2 - A_1 - \cfrac{|B_2|^2}{\left(z^2 - A_2 - \cfrac{|B_3|^2}{z^2 - \cdots}\cdots\right)}} , \tag{2.13}$$

and similar expansions exist for the off-diagonal terms with $\beta \neq \alpha$, or $\vec{l}' \neq \vec{l}$. In the latter case, the coefficient of the term in $1/z^2$ may be seen to vanish. By following the discussion of Haydock *et al.*[12] and using the analogy outlined above, we can construct the coefficients A_n and $|B_{n+1}|^2$ for n up to some finite value. One then must extrapolate the continued-fraction expansion beyond the finite number of terms produced this way. We perform this extrapolation by a method different than that used in Ref. 12 and which produces results of high quality.

There are two important observations for what follows. First of all, infinitesimal translation invariance of the vibrational potential energy tells us that the frequency spectrum of the vibrations of a stable configuration of masses ($\omega_s^2 \geq 0$ for all s) extends down to zero frequency. Thus, in contrast to the situation encountered in some electronic structure calculations, we know the lower bound to the frequency spectrum must be identically zero.

Also, there is a sum rule obeyed by $\rho_{\alpha\beta}(\vec{l}, \vec{l}'; \omega)$. From Eq. (2.8b) combined with Eq. (2.5), we have

$$\int_0^\infty d\omega\, \rho_{\alpha\beta}(\vec{l}, \vec{l}'; \omega) = \delta_{\alpha\beta}\delta_{\vec{l}\vec{l}'} . \tag{2.14}$$

We shall use this as a check on our numerical calculations of $\rho_{\alpha\beta}(\vec{l}, \vec{l}'; \omega)$ by the continued-fraction method.

The physical implication of this sum rule we use is as follows. If $P_\alpha(\vec{l})$ is the momentum of the atom at site $\vec{l}$, then when $k_B T \gg \hbar\omega_M$, with ω_M the maximum vibrational frequency of the lattice, we have

$$\left\langle \frac{P_\alpha^2(\vec{l})}{2M} \right\rangle = \tfrac{1}{2} k_B T \int_0^\infty d\omega\, \rho_{\alpha\alpha}(\vec{l}, \vec{l}; \omega) , \tag{2.15}$$

so for the special case $\alpha = \beta$, $\vec{l} = \vec{l}'$, satisfaction of the sum rule in Eq. (2.8) ensures that the expectation value on the left-hand side of Eq. (2.9) assumes the value required by the equipartition theorem of classical statistical mechanics. We now turn to a discussion of the method of calculating $U_{\alpha\beta}(\vec{l}, \vec{l}'; z)$ by the method of continued fractions.

III. COMPUTER DETERMINATION OF THE COEFFICIENTS A_n AND B_n

It is not a trivial problem to compute the coefficients A_n and B_n needed in the continued-fraction method. While the calculation parallels that used in the electronic structure problem, at first sight the matrix multiplications needed appear too lengthy to be done on the computer available to us (an SDS Sigma 7). We were, however, able to reduce the multiplications to a manageable form. Since our reduction is an essential feature of the calculation, and since it has not been discussed before, to the best of our knowledge, we report on it here in some detail.

We first consider the reduction when the A_n and B_n required to calculate $\rho_{\alpha\alpha}(\vec{l}, \vec{l}; \omega)$ are to be calculated. Later we shall generalize to the case $\rho_{\alpha\beta}(\vec{l}, \vec{l}'; \omega)$, where $\alpha \neq \beta$, $\vec{l} \neq \vec{l}'$. The heart of the calculation lies in finding an ordered and normalized set of basis functions $\{|M\rangle\}$, of which the first $|1\rangle = |\vec{l}\alpha\rangle$, $B_1 = 0$, and $A_1 = \langle 1|\underline{D}|1\rangle$. From this starting point subsequent coefficients may be determined from the recursion relation, with $\underline{D}$ the dynamical matrix,

$$B_{N+1}|N+1\rangle = \underline{D}|N\rangle - B_N|N-1\rangle - A_N|N\rangle . \tag{3.1}$$

The actual procedure by means of which the A_n and B_n are developed from this relation is carefully described by Haydock, Heine, and Kelly.[12]

The important point to note for our purpose is that the time-consuming part of the iteration is in the multiplication of $\underline{D}|N\rangle$. If we cannot simplify this problem, then the multiplication could involve (roughly) multiplying a $3n \times 3n$ matrix with a column vector of size $3n$. Here n is the number of atoms we use, and as we shall see later it must be several thousand for a sufficient number of coefficients A_n and B_n to be generated. Thus we deal with a matrix of order 10^8 elements, and we need to perform about 10^8 multiplications to determine $\underline{D}|N\rangle$.

The multiplications needed can be reduced considerably provided we can exploit two features of the problem. First, note that we do not allow every atom to interact with every other atom. In fact, we allow the tungsten atom to interact with only its first three neighbors (26 atoms for a bcc lattice). This choice was based in part on the fact that in the bulk of the crystal the model gives a frequency distribution which is very similar to that obtained with an eight-neighbor model,[13] and in part on the fact that our preliminary studies showed that a two-neighbor model gave dispersion relations in off-symmetry directions very sensitive to the choice of force constants. We believe the three-neighbor model provides a good description of tungsten lattice dynamics in the bulk, yet involves few enough neighbors that the continued-fraction method can be undertaken. Force constants of Chen and Brockhouse[14] were used to construct the dynamical matrix. With the three-neighbor model only 27 of the elements characterized by $\vec{l}'$ in $D_{\alpha\beta}(\vec{l}, \vec{l}')$ are nonzero for a given choice of $\vec{l}$. Secondly, note that for the $N+1$th iteration there are $n_N \times 3 \times 1$ elements of the vector $|N\rangle$. Since each of these will interact with only 27 (or less) atoms we could, in principle, only perform $3 \times$ (number of neighbors) $\times 3 \times n_N$ multiplications in a given iteration. This number should be compared with $3 \times n \times 3 \times n$, estimated as the worst case, where n is the total number of atoms we wish to work with.

To exploit these ideas we construct a nonsquare matrix $\underline{D}_1'$ whose rows are the atom numbers and whose columns correspond to the 27 interactions (including self-interactions) which any one atom can have with the surrounding atoms. As elements of the matrix we use the atom numbers of the neighbors, or zero if no neighbor exists, such as can occur at the surface of a crystal for example.

The atoms are numbered as follows. We start by assigning 1 to the atom ($\vec{l}$) whose autocorrelation we are interested in. We generate the 26 neighbors systematically, starting with the nearest neighbor in the positive octant, and proceeding. We number the atoms 2, 3, ..., 27. We call these atoms the second shell of atoms. We then proceed to find the neighbors of these 26 atoms, doing each atom in turn. Whenever an atom not previously encountered occurs, it is assigned a new number. Numbers of atoms in the shells of the bulk are 1, 26, 122, 298, 554, 890, 1396, 1802, ..., while the number starting with a surface atom in the (100) plane are 1, 17, 67, 161, 293, 465, 677, 969, 1221, ... Total atoms for the shells shown are 4999 and 3833, respectively.

Since we develop the elements of the given row of the matrix systematically, we may associate with each column the dynamical matrix $D_{\alpha\beta}$ (column) appropriate to the neighbor chosen. Thus to obtain an element of the matrix $B_{N+1}|N+1\rangle$ we multiply each of these 27 3×3 matrices of a row of D_1' with the 3×1 column vectors identified on the elements of the matrix D_1'. One 3×1 element of $B_{N+1}|N+1\rangle$ requires $3 \times 3 \times 27$ multiplications. In fact, there may be less multiplication since, for example, surface atoms have less than 27 neighbors.

In constructing all elements of $B_{N+1}|N+1\rangle$ we then must multiply $|N\rangle$ by the first $N+1$ shells of atoms. Further, atom shells do not interact with the atoms associated with the nonzero elements of N. While this does not cut out all zero-element multiplication, it is an improvement over multiplying by all n atoms of the matrix $\underline{D}_1'$. We find, for example, that for shells of 8 levels, $3 \times 3 \times 2 \times 27 \times n$ multiplications are required. This is a considerable improvement over the $3 \times 3 \times n^2 \times 8$ we would expect from the crudest method with $n = 4999$.

Actual computer CPU times for a typical case are as follows. Four minutes were required to produce $\underline{D}_1'$ in the bulk with 8 shells. Seven minutes were then required to iterate through to A_7 and B_8. The last iteration took two minutes of c.p.u. time. Incidentally, to manipulate the large array $\underline{D}_1'$, with its 27×3197 elements, we used a FORTRAN library routine called PAGE which will handle very large arrays without assigning large amounts of space in the source programs.

We proceed along similar lines if we wish to determine the coefficients needed for $\rho_{\alpha\beta}(\vec{l}, \vec{l}'; \omega)$ when $\beta \neq \alpha$ and $\vec{l} \neq \vec{l}'$. In this case we first construct the matrix $\underline{D}_2'$. This is determined by starting the atom-numbering system with a pair of atoms at $\vec{l}$ and $\vec{l}'$ rather than a single atom at $\vec{l}$. We then obtain a resolvent (R_+) by starting the iteration with $|1\rangle = (1/\sqrt{2})(|\vec{l}, \alpha\rangle + |\vec{l}', \beta\rangle)$ and a second resolvent (R_-) with the starting basis vector $(1/\sqrt{2})(|\vec{l}, \alpha\rangle - |\vec{l}', \beta\rangle)$. The final resolvent density is then given by $\frac{1}{2}(R_+ - R_-)$, and the theory of this is described in Ref. 12.

Since only a finite number of coefficients A_n and

B_n can be calculated exactly with the consequence that only a finite cluster of atoms centered about the site of interest is sampled, some method of extrapolating the continued-fraction expansion to infinity is required. This may be done in various ways, and the ultimate accuracy of the results is influenced by how this is done.

Formally, given A_1 through A_N and B_2 through B_{N+1}, the continued fraction may be terminated by introducing an effective self-energy $T(z^2)$ so that

$$U_{\alpha\alpha}(\vec{l},\vec{l};z)=\cfrac{1}{z^2-A_1-\cfrac{|B_2|^2}{z^2-A_2\cdots-|B_{N+1}|^2T(z^2)}}, \tag{3.2}$$

where the coefficient B_{N+1} is obtained from the Nth shell. As discussed in Ref. 12, if the coefficients (A_n, B_n) are calculated for n sufficiently large that they attain the limiting values A_∞ and B_∞ to sufficient accuracy, then a closed formula for $T(z^2)$ is readily obtained.

If we set $T(z^2)$ equal to zero, then the density of states is a sequence of weighted delta functions. These can be smoothed by giving to z a finite imaginary part to move the poles off the real axis. In effect, each delta function is converted to a Lorentzian of finite width. We found this approach works much less well than use of an appropriate form for $T(z^2)$.

We proceed to find an approximation to A_∞ as follows. By setting $T(z^2)$ equal to zero, an effective phonon bandwidth can be defined as the difference $\omega_M^2-\omega_m^2$, with ω_M and ω_m the position of the highest- and lowest-frequency poles in the approximate form for the continued fraction constructed from A_1 through A_N, and B_2 through B_N. We find this effective bandwidth converges well as N increases. We illustrate this for bulk tungsten in Fig. 1, where we plot the square of the effective bandwidth just defined against N. As $N\to\infty$, this effective square of the bandwidth must converge to $4B_\infty$, which should also equal $2A_\infty$, because the phonon spectrum extends down to zero frequency. From plots such as Fig. 1, we thus obtain estimates of both A_∞ and B_∞. In fact, we find always that for $N>5$, the estimated A_∞ and B_∞ change by less than ten percent as N is increased. Given such values of A_∞ and B_∞, we then calculate $T(z^2)$ through use of the procedure of Haydock *et al.*[12]

Errors in A_∞ and B_∞ of a few percent seem to have little serious qualitative influence on the results. For example, we found that the sum rule in Eq. (2.14) was obeyed to one part in one thousand for the terminations used. Only if we shifted A_∞ deliberately well away from its asymptotic values was the sum rule violated by more than 0.5%.

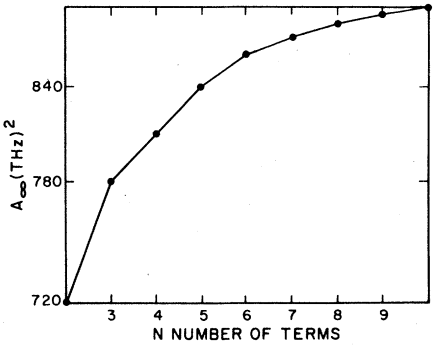

FIG. 1. We plot the effective phonon bandwidth, as defined in Sec. III of the text, as a function of the number of iterations N in the continued-fraction method. The figure applies to the bulk of tungsten.

We give a test of the accuracy of our procedure in Fig. 2. Chen[13] has calculated the bulk phonon density of states for tungsten by the Gilat-Raubenheimer method, which is a $\vec{k}$-space summation procedure. The force-constant model we are using here is identical to that used by Chen, thus a direct comparison of our calculations with Chen's is possible. The dots in Fig. 2 are selected points from Chen's calculation, and the solid line is our bulk phonon density of states. The two calculations are in remarkable agreement. We have used seven shells of atoms for the particular calculation, though results of comparable accuracy can be found from only six shells. Thus, for all of the calculations reported in Sec. IV, we have used six shells. In our experience, there is no simple quantitative procedure for deciding how many shells are needed in the calculation. The important point is to establish whether adding further shells alters the feature or features of interest in any specific instance. In Sec. IV, we turn to a discussion of vibratory motions of atoms in and near a (100) surface of the model crystal.

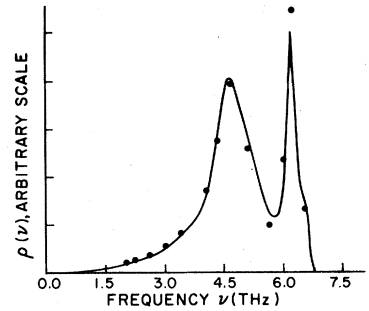

FIG. 2. A comparison between the bulk phonon density of states calculated by the continued-fraction method (solid line) and by a direct $\vec{k}$-space summation method as carried out by Chen (dots).

IV. STUDIES OF ATOMIC MOTION IN AND NEAR THE SURFACE

In Fig. 3, we show the mean-square displacement of surface and bulk tungsten atoms along with the associated spectral densities. In Fig. 3(a) we show the mean-square displacement $\langle u_x^2\rangle_b$ of a bulk tungsten atom as a function of temperature, while Fig. 3(b) gives the spectral density $\rho_{xx}(\vec{l}_b, \vec{l}_b; \omega)$ for an atom deep in the bulk. As remarked earlier, $\rho_{xx}(\vec{l}_b, \vec{l}_b; \omega)$ is simply equal to the bulk phonon density of states (Fig. 2) far from the surface.

Figure 3(c) gives the normal component of the mean-square displacement $\langle u_z^2\rangle_s$ for an atom in the surface, while the associated spectral density is displayed in Fig. 3(d). First of all, as found commonly in such studies, the surface mean-square displacement is substantially larger than in the bulk.[1] For our model, at a temperature of 400 K, we have $\langle u_x^2\rangle_b = \langle u_y^2\rangle_b = \langle u_z^2\rangle_b = 2.62 \times 10^{-19}$ cm^2 while at the same temperature $\langle u_z^2\rangle_s = 5.63 \times 10^{-19}$ cm^2. These results agree well with earlier calculations by Wallis and Cheng,[15] and also with results obtained earlier by Dobrzynski and Masri.[16]

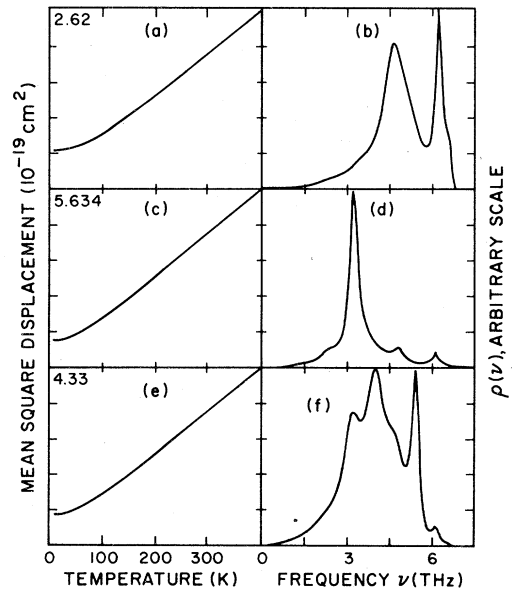

FIG. 3. We show (a) the mean-square displacement $\langle u_x^2\rangle = \langle u_y^2\rangle = \langle u_z^2\rangle$ calculated for a bulk tungsten atom combined with (b) the bulk phonon density of states. We compare this with (c) the mean-square displacement $\langle u_z^2\rangle_s$ of a surface atom normal to the surface and (d) its associated spectral density, and also with (e) the mean-square displacement component $\langle u_x^2\rangle_s$ of a surface atom parallel to the surface along with (f) its spectral density. The numbers in the upper left corner are values of the relevant mean-square displacements at 400 K, in units of 10^{-19} cm^2.

All three studies used somewhat different models of the lattice dynamics of the bulk material, and the ratio $\langle u_z^2\rangle_s/\langle u_z^2\rangle_b$ seems rather insensitive to the model.

It is most instructive to examine the spectral density $\rho_{zz}(\vec{l}_s, \vec{l}_s; \omega)$ for the surface atom as shown in Fig. 3(d). The surface spectral density is dominated by a single, prominent peak which lies below both features in the bulk phonon density of states. This peak has its origin in a Rayleigh surface wave which propagates along the [100] direction. For the model, we have calculated the frequency of the zone-boundary Rayleigh wave in this direction to find 3.27×10^{12} Hz, in excellent accord with the prominent peak in Fig. 3(d). From Eq. (2.9) combined with the sum rule in Eq. (2.14), one sees that the enhanced mean-square displacement in the surface requires spectral weight to be shifted downward in $\rho_{zz}(\vec{l}_s, \vec{l}_s; \omega)$; in the case of motion normal to the surface, the bulk phonon features have almost disappeared to leave the single low-frequency structure from the Rayleigh surface wave, and the physical mechanism responsible for the enhanced mean-square displacement is clear.

We show the temperature variation of $\langle u_x^2\rangle_s$ in Fig 3(e) and the spectral density $\rho_{xx}(\vec{l}_s, \vec{l}_s; \omega)$ in Fig. 3(f). For motion parallel to the surface, we have $\langle u_x^2\rangle_s = 4.33 \times 10^{-19}$ cm^2 at 400 K, a value intermediate between the bulk value and that associated with motion parallel to the surface. The spectral density $\rho_{xx}(\vec{l}_s, \vec{l}_s; \omega)$ contains prominent structure in the frequency regime where the bulk phonon density of states is largest. A feature near the zone-boundary Rayleigh wave frequency is evident, but the sum rule requires its integrated strength to be very much smaller than that in $\rho_{zz}(\vec{l}_s, \vec{l}_s; \omega)$. A consequence is that $\langle u_x^2\rangle_s$ is substantially smaller than $\langle u_z^2\rangle_s$. Our value for $\langle u_x^2\rangle_s$ is roughly ten percent smaller than that obtained by Wallis and Cheng. We attribute this to differences in the lattice-dynamical models used in the work.

The results for the surface spectral densities are consistent with a picture in which the "important" bulk phonons (those responsible for the structure in the bulk phonon density of states) have a normal component of displacement that suffers a nearly 180° phase shift upon striking the surface, producing an eigenvector with nearly zero amplitude there. The parallel component is reflected with no change of sign. We then require a strong surface wave component in $\rho_{zz}(\vec{l}_s, \vec{l}_s; \omega)$ and a much reduced one in $\rho_{xx}(\vec{l}_s, \vec{l}_s; \omega)$ to maintain the sum rule.

While our calculation is carried out for a model of the W (100) surface and the experiment of Ibach

and Bruchmann cited in Sec. I has been carried out on Ni (111), our calculation bears a striking resemblance to their data and the interpretation these authors have offered of it. They find a prominent peak in their near-specular EELS spectrum of Ni (111) with frequency below the maximum vibrational frequency of bulk Ni, and with frequency only weakly influenced by adsorbed overlayers of various kinds. They argue the feature is produced by a zone-boundary Rayleigh wave of the substrate. Such modes can be observed near the specular when the substrate is covered by an ordered overlayer with a 2×2 structure. If the near-specular scattering is assumed to be dipole scattering enhanced by adsorption of strongly electronegative species in a 2×2 structure, then the theory of dipole scattering suggests that the normal component of atomic displacement[17] should be responsible for the scattering. Quite clearly, the spectral densities displayed in Figs. 3(d) and 3(f) are consistent with such an interpretation. Atomic motions parallel to the surface have a rich and complex spectral composition, while those normal to the surface are dominated by the Rayleigh surface waves near the zone boundary, as Ibach and Bruchmann suggest. Calculations of the surface spectral densities are currently underway for the Ni (111) surface to see if similar results follow for that surface also. We note that in a recent perprint, Allan and Lopez have studied surface vibrations of Ni (111) based on a lattice-dynamical model deduced from a model electronic band structure.[18] A discussion of their work and its relation to the lattice-dynamical models such as those used here will be deferred until our study of the Ni (111) is complete.

This is another implication of the result we wish to mention. In a recent paper, Rahman and Mills[19] have examined the coupling of electrons to substrate phonons when the electrons are trapped in image-potential bound states. The aim of the analysis is to explore the influence of electron-phonon coupling on LEED fine structures which has been interpreted by McRae[20] as having origin in long-lived image-potential-induced resonances. Rahman and Mills assume that an electron outside the crystal couples to substrate phonons via modulation of the image potential by the ripple produced in the surface by a phonon. In fact, they considered only the rippled produced by Rayleigh surface waves and ignored bulk phonon contributions to it. We see here that the bulk phonons indeed play a minor role in modifying the surface profile, and the present calculation offers support for this one feature of the analysis of Rahman and Mills.

In Fig. 4 we show the variation of $\rho_{zz}(\vec{l},\vec{l};\omega)$ with distance from the surface. In both the surface and first layer below it, we have substantial deviations of the spectral density from bulk behavior, although by the second layer below the surface layer the spectral density is settling down to its bulk value. As we see from Fig. 5, $\rho_{xx}(\vec{l},\vec{l};\omega)$ assumes a form rather similar to the bulk even in the first layer below the surface. The information in Figs. 3–5 may be loosely summarized by the statement that the motion normal to the surface is perturbed much more strongly by the presence of the surface than the parallel motion. This is evident from the previously established fact[1] that $\langle u_z^2\rangle_s > \langle u_x^2\rangle_s$; the spectral-density plots provide one with a picture of the physical origin of this behavior.

We turn next to a discussion of correlations between the motions of atoms in and near the surface, i.e., to the behavior of the correlation functions $\langle u_\alpha(\vec{l})u_\beta(\vec{l}')\rangle_s$ for $\vec{l}'\neq\vec{l}$. There are two reasons why such correlation functions are of interest. First of all, we can ask if the pattern of atomic motions in the surface layer differs qualitatively from those in the bulk. We might expect less correlation between the motion between adjacent atoms in the surface than between a pair of bulk atoms with similar relative position. This may be so simply because surface atoms couple to fewer neighbors than bulk atoms. Qualitative pictures of the correlation between atomic motions, with attention to such questions, may prove useful for a variety of reasons. We are also

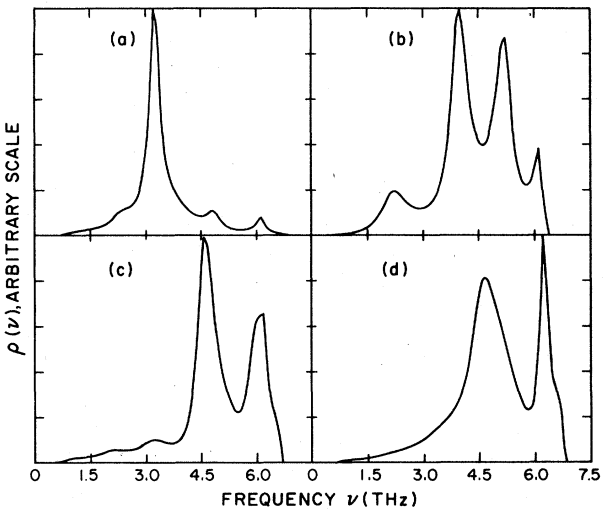

FIG. 4. The local spectral density $\rho_{zz}(\vec{l},\vec{l};\omega)$ for atomic motions normal to the surface as a function of distance from the surface. We see that in the fourth layer below the surface, $\rho_{zz}(1,1;\omega)$ has settled down to its bulk behavior.

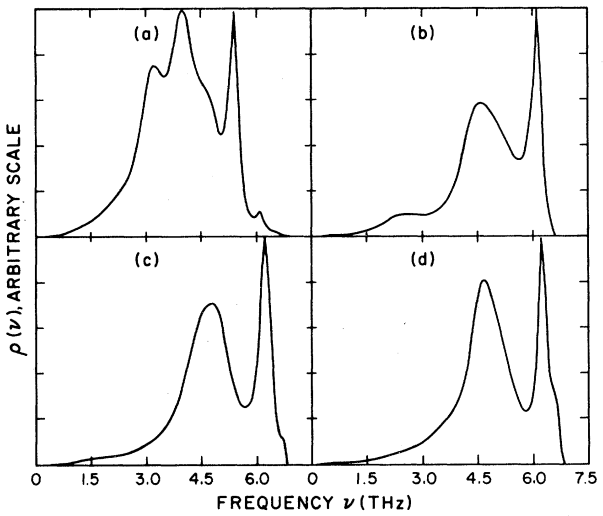

FIG. 5. The local spectral density $\rho_{xx}(\vec{l},\vec{l};\omega)$ for atomic motions parallel to the surface as a function of distance from the surface. Even in the second layer $\rho_{xx}(\vec{l},\vec{l};\omega)$ assumes a form very similar to the bulk phonon density of states.

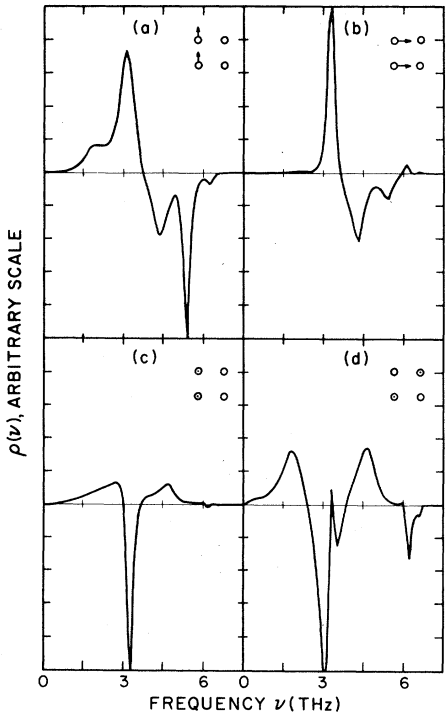

FIG. 6. In (a) through (d), we show the spectral density which controls correlation functions of the form $\langle u_\alpha(\vec{l})u_\alpha(\vec{l}')\rangle$, for various combinations of $\vec{l},\vec{l}'$ and α. In (c) and (d) we give spectral densities for motion parallel to the surface.

interested in directing our attention to a proper theory of thermal diffuse scattering, where multiple scattering of electrons from the substrate is included fully, as in the recent theory of large-angle EELS.[21,22] Correlation functions of the above-mentioned form are an essential component of the theory of thermal diffuse scattering.[1]

In Fig. 6(a), we show the correlation function and the spectral density associated with the correlation function $\langle u_y(\vec{l})u_y(\vec{l}')\rangle_s$ for the neighbors arranged as indicated in the inset. The sum rule requires the area under the curve to vanish, so the spectral density is oscillatory in character in contrast to those associated with autocorrelation functions which are necessarily positive definite. The prominent positive peak lies near but not coincident with the Rayleigh wave frequency discussed earlier. We believe this comes from a shear polarized surface wave we find at the two-dimensional zone boundary in the [100] direction. The frequency of this wave, which is a bit below the Rayleigh wave at the zone boundary, agrees well with the position of our calculated peak, and such a shear polarized mode propagating along $\hat{x}$ would drive the two atoms in parallel motion. A complete study of the dispersion relation of the surface modes for our model would prove a most useful aid in interpreting the structures in the spectral densities. We hope to turn to such a study shortly.

In Fig. 6(b), we show the spectral density of $\langle u_x(\vec{l})u_x(\vec{l}')\rangle_s$, and in Fig. 6(c) we give that for $\langle u_z(\vec{l})u_z(\vec{l}')\rangle_s$ for the same pair of atoms chosen to generate Fig. 6(a). The large sharp negative peak in Fig. 6(c) comes from the zone-boundary Rayleigh wave, which sets nearest neighbors into antiparallel motion. We believe the strong low-frequency peak in $\langle u_x(\vec{l})u_x(\vec{l}')\rangle_s$ comes from the Rayleigh wave, which when propagating along [100] drives the two atoms in parallel motion. Right at the zone boundary, an analytic study shows the Rayleigh wave to be z polarized. Thus, this feature in the spectral density must have its origin in a critical point in the dispersion relation away from the zone boundary. Again, a study of surface-wave dispersion curves for the model will prove useful.

We have attempted to interpret the structures in the spectral densities to see to what extent a small number of surface modes can be isolated and regarded as providing the dominant contribution to the spectral densities. In essence, the question is whether one can account for the mean-square displacements and nearest-neighbor correlations in a semiquantitative fashion by this means. The situation in fact appears complex, with a variety of different modes, including bulk phonons, contributing importantly. There are numerous papers in the literature which calculate vibrational con-

tributions to the free energy and surface entropy through use of an Einstein model of surface vibrations.[23] In essence, from the diagonal elements of the dynamical matrix, effective Einstein frequencies are determined and used in the evaluation of the surface contributions to the thermodynamic functions. One obtains by this method the leading term of a moment expansion of the thermodynamic potential. The series converges rather rapidly, and by this means one obtains reliable semiquantitative estimates of model predictions of the surface contributions to the thermodynamic properties. We see it is misleading to take the next step and assume the Einstein frequencies so calculated have any connection with the actual frequency spectrum of atomic vibrations in the surface.

Finally, we see in Fig. 6(d) that when we consider second-nearest neighbors, the spectral density contains rather complicated oscillatory structure. This is expected, because if one writes out the explicit form of $\langle u_\alpha(\vec{l})u_\beta(\vec{l}')\rangle$ in a representation that recognizes $\vec{k}_\parallel$ is a good quantum number, then a factor of $\exp[i\vec{k}_\parallel\cdot(\vec{l}_\parallel-\vec{l}'_\parallel)]$ appears in the integrand. As $\vec{l}_\parallel$ and $\vec{l}'_\parallel$ are separated, this exponential factor oscillates more and more rapidly when considered a function of $\vec{k}_\parallel$. We believe the present method cannot be extended beyond second neighbors to obtain reliable results without including a very large number of atoms in the basic cluster. We have no reason to doubt the second neighbor results, however. If one desires to study correlations between atoms at larger separations, one may need to use elasticity theory, which can be joined to a lattice-dynamical picture like the present method when the separation between $\vec{l}$ and $\vec{l}'$ is small.

The last remark does not imply the continued-fraction method is not useful in the theory of thermal diffuse scattering, where correlations beyond second neighbors are clearly required. The theory of thermal diffuse scattering can be cast in terms of Fourier transforms of the form

$$F_{\alpha\beta}(\vec{k}_\parallel; l_z, l'_z)=\sum_{\vec{l}'_\parallel}\exp[i\vec{k}_\parallel\cdot(\vec{l}_\parallel-\vec{l}'_\parallel)]\langle u_\alpha(\vec{l})u_\beta(\vec{l}')\rangle\,. \tag{4.1}$$

The continued-fraction method may be used to calculate these directly from the Fourier-transformed dynamical matrix

$$D_{\alpha\beta}(\vec{k}_\parallel; l_z, l'_z)=\sum_{\vec{l}'_\parallel}\exp[i\vec{k}_\parallel\cdot(\vec{l}_\parallel-\vec{l}'_\parallel)]D_{\alpha\beta}(\vec{l},\vec{l}')\,. \tag{4.2}$$

We have calculated selected correlation functions of the form $F_{\alpha\beta}(\vec{k}_\parallel; l_z, l'_z)$ by the continued-fraction method for a simple analytically soluble model; the continued-fraction method works remarkably well to the point where the square-root singularities that occur in these quasi-one-dimensional correlation functions[11] show up very nicely. We shall describe such calculations in detail elsewhere.

We turn next to the question raised earlier regarding a comparison between the degree of correlation in the surface and the bulk. Consider correlation in the x displacement between the nearest-neighbor pair as shown in Fig. 6(b). For such a pair located in the surface layer, we find $\langle u_x(\vec{l})u_x(\vec{l}')\rangle/\langle u_x^2\rangle_s=0.40$, while for a similar pair located in (100) plane far into the bulk we find $\langle u_x(\vec{l})u_x(\vec{l}')\rangle/\langle u_x^2\rangle_b=0.27$. Similarly, for the same pair in the surface $\langle u_z(\vec{l})u_z(\vec{l}')\rangle_s/\langle u_z^2\rangle_s=0.184$, while in the bulk $\langle u_z(\vec{l})u_z(\vec{l}')\rangle_s/\langle u_z^2\rangle_b=0.17$. The calculations show that motions of nearby atoms in the surface are correlated to very much the same degree as in the bulk; indeed, the xx correlation function cited above is actually substantially larger.

We conclude by presenting the result of one final inquiry into the nature of vibrational motion in the surface. Consider an isolated planar molecule made from four identical nuclei arranged on the corners of a square. One normal mode of the molecule will be the fully symmetric breathing mode in which each atom moves outward along the diagonal. If we examine four molecules which form a square within the surface layer, we can ask if the breathing motion can be approximated by a single frequency, much as if it retained some remnant of its molecular character after being embedded in the surface. It has been suggested that an answer to this question may be helpful in understanding the mechanism that controls diffusion of atoms into the bulk of crystals.[24]

We may address this question by choosing four atoms in the surface that form a square, and then forming the normal coordinate $Q=u_r(\vec{l}_1)+\cdots+u_r(\vec{l}_4)$, where $u_r(\vec{l}_i)$ is the component of atomic displacement along the diagonal of the square, chosen positive for outward motion. We then calculate the spectral density $\rho_{QQ}(\omega)$ associated with the quantity $\langle Q^2\rangle$. This may be written as a linear combination of nearest- and next-nearest-neighbor correlation functions. The result is displayed in Fig. 7 along with the temperature variation of the average $\langle Q^2\rangle$, which assumes the value 5.4×10^{-19} cm^2 at 400 K. We see a rich variety of structures in $\rho_{QQ}(\omega)$; this quantity receives contributions from a variety of short-wavelength surface and bulk phonons, and there is no obvious remnant of a quasi-molecular breathing vibration.

One may easily prove that $\rho_{QQ}(\omega)$ must be posi-

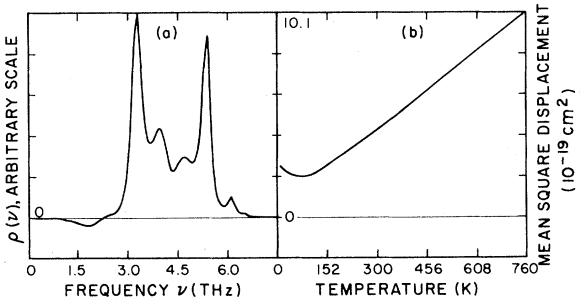

FIG. 7. (a) The spectral density $\rho_{QQ}(\omega)$ which contains the frequency spectrum of the breathing vibrations of a square of atoms embedded in the crystal surface, and (b) the temperature variation of $\langle Q^2 \rangle$, where Q is the normal coordinate of the square.

tive definite. One sees a small region in Fig. 6(a) where this quantity becomes negative. This is an error in our calculation. As we have seen, the next-nearest-neighbor correlation functions oscillate rather dramatically, and one may introduce some error by truncating the sequence of A_n's and B_n's as we have described above. It is hard to remedy the problem without a substantial cost in computer time, since more shells must be included in the basic cluster. The error creeps in at low frequencies, where we have least confidence in the method. The nonmonotonic behavior of $\langle Q^2 \rangle$ in Fig. 6(b) is caused by this unphysical negative dip in $\rho_{QQ}(\omega)$, incidentally. The integrated area associated with the region where $\rho_{QQ}(\omega)$ is negative is a small fraction of the total, and in this sense we do not regard the problem as serious. We have deliberately displayed the curve with the problem clearly present to provide the reader with an appreciation of the limitations in the method.

The aim of this paper has been to explore application of the method of continued fractions to the problem of surface lattice dynamics and also to provide physical insight into the nature of atomic motions in surface. We are pleased with the results, and we plan to apply the technique to the study of vibrations at and near localized defects on the surface, such as isolated adsorbates and steps. Here we believe the continued-fraction method offers a distinct advantage over the slab methods described in Sec. I.

ACKNOWLEDGMENTS

We are most grateful to Professor R. F. Wallis for numerous helpful discussions during the course of this work and also for providing us with the details of his work on the W (100) surface performed in collaboration with D. J. Cheng. This research was supported by the Department of Energy through Contract No. DE-AT0379-ER10432. One of us (B.L.) is partially supported by CNPq (Conselho Nacional de Desenvolvimento Cientifico e Tecnologic Brasil).

---

*On sabbatical leave from the Dept. of Physics, Brock University, St. Catharines, Ontario, Canada, L2S 3A1.

†On leave from the Dept. of Physics, Universidade Estadual de Campinas (UNICAMP), 13100 Campinas, Brazil.

[1]For a comprehensive review of the literature on surface lattice dynamics, see the review article by R. F. Wallis, Prog. Surf. Sci. 4, 233 (1973).

[2]See the discussion that begins on p. 296 of Ref. 1 and the calculation of T. S. Chen, G. P. Alldredge, F. de Wette, and R. E. Allen, J. Chem. Phys. 55, 3121 (1971), which agrees impressively with data on the surface specific heat of NaCl.

[3]See the discussion presented by C. B. Duke and G. E. Laramore, Phys. Rev. B 2, 4765 (1970); G. E. Laramore and C. B. Duke, *ibid.* 2, 4783 (1970).

[4]See the review articles by H. Froitzheim, in *Topics in Current Physics*, edited by H. Ibach (Springer, New York, 1976), Vol. 4, and D. L. Mills, Prog. Surf. Sci. 8, 143 (1977).

[5]H. Ibach, Phys. Rev. Lett. 24, 1416 (1970); 27, 253 (1971).

[6]H. Ibach and D. Bruchmann, Phys. Rev. Lett. 44, 36 (1980).

[7]F. Cyrot-Lackmann, Surf. Sci. 15, 539 (1969); F. Cyrot-Lackmann and F. Ducastelle, J. Phys. Chem. Solids 31, 1295 (1970); F. Cyrot-Lackmann, M. C. Desjonqueres, and J. P. Gaspar, J. Phys. C 7, 925 (1974); R. Haydock, V. Heine, and M. J. Kelly, J. Phys. C 5, 2845 (1972); 8, 2591 (1975).

[8]An exception is the work of Mostoller and Landman. See M. Mostoller and Uzi Landman, Phys. Rev. B 20, 1755 (1979).

[9]As far as we know, the slab method was introduced by R. F. Wallis, D. L. Mills, and A. A. Maradudin, in *Localized Excitations in Solids*, edited by R. F. Wallis (Plenum, New York, 1968), p. 403.

[10]Actually, for a slab of planes with all three degrees of freedom $u_x(\vec{l})$, $u_y(\vec{l})$, and $u_z(\vec{l})$ allowed for each atom, the divergence is stronger than for the textbook example of a plane of atoms with displacements confined to the plane. When $u_z(\vec{l})$ is allowed to be nonzero in the long-wavelength limit $|\vec{k}_{\parallel}|d \ll 1$, with d the slab thickness and $\vec{k}_{\parallel}$ the wave vector of the phonon, the transverse acoustical phonon branch with $u_z(\vec{l})$ nonzero describes a buckling motion of the whole slab. The dispersion relation assumes the form $\omega(\vec{k}_{\parallel}) = Ak_{\parallel}^2$ in this regime, and the density of low-lying modes is very much larger than for acoustical phonons with $\omega(\vec{k}_{\parallel}) \sim k_{\parallel}$. The influence of the buckling modes on the mean-square displacement of atoms in a slab, and the nature

of the divergence they produce, has been discussed by Portz and Maradudin. See K. A. Portz, thesis, University of California at Irvine, 1978 (unpublished), and K. A. Portz and A. A. Maradudin (unpublished).
[11]V. Roundy and D. L. Mills, Phys. Rev. B 5, 1347 (1972).
[12]See the 1975 paper by Haydock *et al.*, cited in Ref. 7.
[13]S. H. Chen, Ph.D. thesis, McMaster University, 1964 (unpublished).
[14]S. H. Chen and B. N. Brockhouse, Solid State Commun. 2, 73 (1964).
[15]R. F. Wallis and D. J. Cheng (unpublished).
[16]L. Dobrzynski and P. Masri, J. Chem. Phys. Solids 33, 1603 (1972).
[17]E. Evans and D. L. Mills, Phys. Rev. B 5, 4126 (1972); D. L. Mills, Prog. Surf. Sci. 8, 143 (1977).
[18]G. Allan and J. Lopez, Surf. Sci. (in press).
[19]Talat S. Rahman and D. L. Mills, Phys. Rev. B 21, 1432 (1980).
[20]E. G. McRae, Rev. Mod. Phys. 51, 541 (1979).
[21]C. H. Li, S. Y. Tong, and D. L. Mills, Phys. Rev. B 21, 3057 (1980).
[22]S. Y. Tong, C. H. Li, and D. L. Mills, Phys. Rev. Lett. 44, 407 (1980).
[23]See, for example, D. Djafari-Rouhani, L. Dobrzynski, and G. Allan, Surf. Sci. 55, 663 (1976).
[24]R. Madix (private communication).